

Spin Fine Structure in Optically Excited Quantum Dot Molecules

M. Scheibner,^{1*} and M. F. Doty,¹ I. V. Ponomarev¹, A.S. Bracker¹,
 E.A. Stinaff¹, V.L. Korenev², T.L. Reinecke,¹ D. Gammon¹
¹*Naval Research Laboratory, Washington, DC 20375, USA* and
²*A.F. Ioffe Physical Technical Institute, St. Petersburg 194021 Russia*

(Dated: December 2, 2024)

The interaction between spins in coupled quantum dots is revealed in distinct fine structure patterns in the measured optical spectra of InAs double quantum dot molecules containing zero, one, or two excess holes. The fine structure is explained well in terms of a unique molecular interplay of spin exchange interactions, Pauli exclusion and orbital tunneling. This knowledge is critical for converting quantum dot molecule tunneling into a means of optically coupling not just orbitals, but spins.

PACS numbers: 78.67.Hc, 73.21.La, 78.47.+p, 78.55.Et

Exchange coupling between spins in a double quantum dot molecule (QDM) is an essential component for spin-based quantum information [1, 2, 3]. Rapid progress has been made over the last year in doubly charged QDM's that are measured and controlled electrically [4, 5]. A corresponding understanding of the spin-spin interactions in optically controlled QDMs is not yet available. These systems could lead to ultrafast, wireless control of spin qubits. To this end it is now critical to obtain a detailed measurement and understanding of the spin states of optically excited QDM's.

In optically excited dots, an electron-hole (e - h) pair is created in the presence of the previously existing spin(s). As we will show, the resulting e - e , h - h , and e - h exchange interactions determine the spin states and can be directly measured through fine structure in the spectra [6, 7]. Moreover, e 's or h 's may be coupled by carrier tunneling in a QDM, with the orbital wavefunctions continuously tuneable from atomic to molecular in nature [8, 9, 10].

Of great importance is the case of a doubly charged QDM because of its potential use as a two qubit system. To understand this system, we examine cases of zero, one and two charges in the QDM. We demonstrate that all of the fine structure features of these systems arise from different combinations of the fundamental quantum mechanical processes - tunneling, exchange and Pauli exclusion. The exciton and biexciton in an uncharged QDM illustrate each of these processes independently. For the singly charged exciton we find that the interplay of all these processes leads to a highly intriguing behavior. We apply these results to the case of two spins in a double quantum dot, a system that can provide an optically controlled two qubit system.

Photoluminescence (PL) spectra of vertically-stacked InAs/GaAs QDMs measured as a function of electric field have recently led to the clear identification of tunnel coupling in neutral [8, 9, 10] and charged QDMs [10]. Our QDMs were designed to exhibit hole level resonances when embedded in an electric field tunable heterostructure and were grown with wide interdot barriers of $d \geq 4$

nm. A Titanium-Sapphire laser was used to excite the QDMs below the energy of the wetting layer. The overall spectral resolution of our PL setup was $50 \mu\text{eV}$. A superconducting split coil magnet was used for magnetic field studies. All experiments were performed at 10 K [11].

To describe the quantum states of a QDM we use, for example $_{21}^{10}X^{2+}$ for a doubly positively charged exciton, where the superscripts on the left are for the e 's and the subscripts are for the h 's, i.e., 1 e and 2 h 's in the bottom dot (B) and 0 e and 1 h in the top dot (T). Likewise $_{21}^{10}X^{2+}$ corresponds to the indirect transition, $_{21}^{10}X^{2+} \Rightarrow _{20}^{00}h^{2+}$. We label specific spin states of a charge configuration as, e.g., $_{\uparrow\downarrow,\uparrow}^{1,0}X^{2+}$, where we use the fact that a h in the ground state of a QD can take only two spin projections ($\uparrow, \downarrow \equiv \pm 3/2$), similar to the case of the spin-1/2 e (\uparrow, \downarrow) [12]. We specify the h spin singlet and triplet configurations as, e.g., $_{\uparrow\downarrow}^{1,0}X_S^+$ and $_{\uparrow\downarrow}^{1,0}X_T^+$ [13]. We will not list spin degenerate states in which all spins, including the e spin, are flipped. The e 's and h 's are treated as non-identical particles with an explicit exchange interaction between them.

We consider first the case of e - h exchange for a single e - h pair in an uncharged dot (the neutral exciton, $X^0 \equiv 1e + 1h$) (Fig. 1). The exciton has spin states that are optically allowed (bright, e.g. $\uparrow\downarrow$), or optically forbidden (dark, e.g. $\uparrow\uparrow$). At zero magnetic field a single intradot exciton line anticrosses with the relatively weak interdot transition with a splitting of $\Delta_{X^0} = 1.0 \text{ meV}$ (Fig. 1(a) top). When a transverse magnetic field of $B = 6 \text{ T}$ is applied (Voigt geometry) a second, normally dark, intradot spectral line appears $320 \mu\text{eV}$ lower in energy (Fig. 1(a) bottom), because the transverse magnetic field mixes the bright and dark states [14]. The intradot exciton, $_{10}^{10}X^0$, is similar to the case of a single dot, and the bright-dark splitting comes from e - h exchange. As the intradot exciton evolves into the interdot exciton, the splitting decreases substantially. This is reproduced by calculations of the energy level structure as seen in Fig. 1(b), which consider e - h exchange only for the intradot configurations $_{10}^{10}X^0$ where one e and one h occupy the

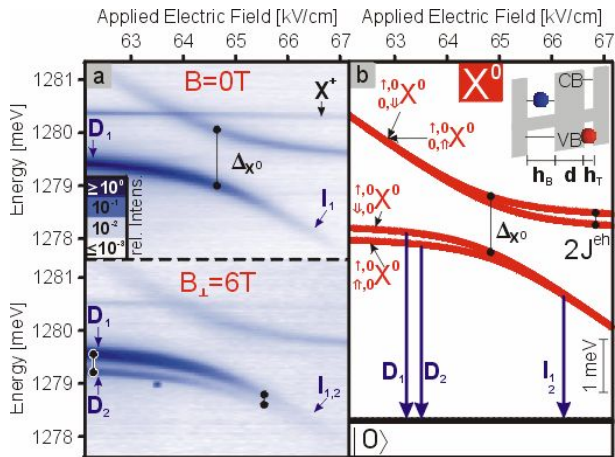


FIG. 1: (Color online) Exciton (X^0) in an uncharged QDM ($h_B = h_T = 2.5$ nm, $d = 4$ nm). (a) The PL spectrum as a function of electric field - at zero magnetic field ($B = 0$) (top) and in a transverse magnetic field ($B = 6$ T) (bottom) (b) The calculated energy diagram ($\Delta_{X^0} = 2t_h = 1.05$ meV, $2J^{eh} = 240$ μ eV). The direct exciton and its corresponding transition ($D_{1,2} \equiv \frac{1}{10}X^0$) has the h in the same dot as the e and its energy is almost independent of electric field, while the indirect exciton ($I_{1,2} \equiv \frac{1}{01}X^0$) has the h in the opposite dot and its energy changes linearly with field. An anticrossing occurs when their energies are resonant.

bottom dot. Here the Hamiltonians of the bright and dark excitons at zero magnetic field are

$$\hat{H}_{b(d)}^{X^0} = \begin{pmatrix} \pm J^{eh} & t_h \\ t_h & -\gamma F \end{pmatrix}, \quad (1)$$

where energy and field are relative to the center of the exciton anticrossing and t_h is the single h tunneling rate [15]. The applied electric field, F , changes the h energy in the top QD by $\gamma F = e(d + (h_B + h_T)/2)F$ (e is the elementary charge, d is the separation of the dots and h_B , h_T are the heights of the dots). In the interdot configuration, $\frac{1}{01}X^0$, e - h exchange is strongly reduced because of the exponentially decreasing e and h wavefunctions. Thus, in a QDM exchange depends strongly on the orbital configuration of the optically excited state.

When we have two or more e 's (or h 's) we must also consider e - e (or h - h) interactions. The case of two e 's has been discussed for dots controlled by electrical gating [4, 5, 16]. The case of two h 's is qualitatively the same and is observed optically in the biexciton (XX^0), i.e. two e 's and two h 's in an uncharged QDM. In contrast to the exciton, the biexciton transition shows an 'x'-pattern with four anticrossings that involve two direct (A and D) and two indirect transitions (B and C), as seen in Fig. 2(a). The transition pattern is understood using the calculated energy diagrams for the initial biexciton state and the final exciton state left after recombination (Fig. 2(b)). The Hamiltonian for the two relevant singlet

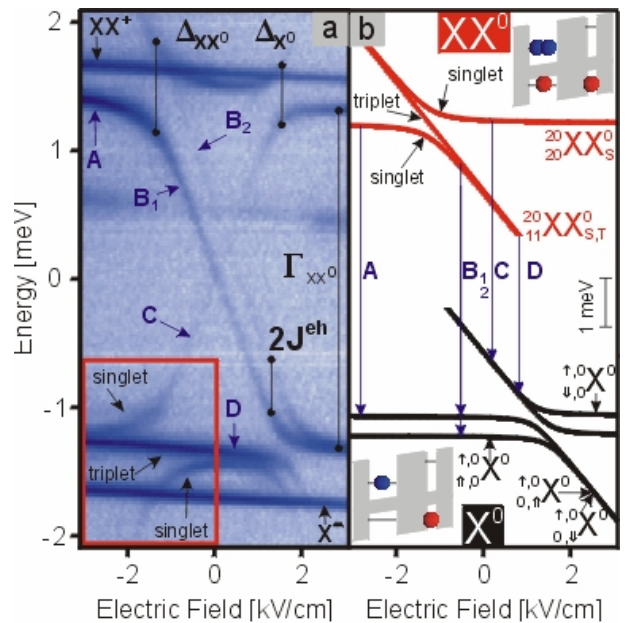


FIG. 2: (Color online) Biexciton (XX^0) in an uncharged QDM ($h_B = h_T = 2.5$ nm, $d = 6$ nm) (a) In the measured PL spectrum as a function of electric field an 'x'-shaped pattern is formed by the XX^0 transitions, $A \equiv \frac{2}{20}XX^0$, $B \equiv \frac{2}{11}XX^0$, $C \equiv \frac{1}{11}XX^0 \rightarrow \frac{1}{01}X^0$ and $D \equiv \frac{2}{11}XX^0$. (b) The calculated level diagram contains the states of the neutral biexciton (XX^0) (red lines) and the states of the neutral exciton (X^0) from Fig. 1(b) (black lines) ($\Delta_{X^0} = 2t_h = 440$ μ eV, $\Delta_{XX^0} = 2\sqrt{2}t_h = 650$ μ eV, $2J^{eh} = 400$ μ eV, $\Gamma_{XX^0} = 2.73$ meV). The two different field dependences seen in the exciton and biexciton states lead to the field-independent direct (A and D) and field-dependent indirect (B and C) PL transitions. B is split by the e - h exchange J^{eh} of the final state (X^0). The red box in (a) marks an area where the singlet-triplet splitting of the XX^0 resonance in (b) is reproduced nicely by the PL-signal. The anticrossing appears rotated because the final state in the transitions (D and C) is field-dependent. In the upper left corner of (a) the anticrossing is reproduced by the transitions A and $B_{1(2)}$ with modifications because of the split final state and optical selection rules.

states of the biexciton is

$$\hat{H}_S^{XX^0} = \begin{pmatrix} E_{XX^0} & \sqrt{2}t_h \\ \sqrt{2}t_h & E_{BT} \end{pmatrix}, \quad (2)$$

where E_{XX^0} is the energy of $\frac{2}{20}XX_S^0$ and $E_{BT} = E_{XX^0} - \Gamma_{XX^0} - \gamma F$ is the field dependent energy of the singlet, $\frac{2}{11}XX_S^0$. The energy of the three decoupled triplet configurations, $\frac{2}{11}XX_T^0$, is also E_{BT} . Γ_{XX^0} is the energy difference of the two direct transitions (A and D) as defined in Fig. 2(a). The two anticrossings on the right in the spectrum of Fig. 2(a) arise from the exciton (Δ_{X^0}) and those on the left from the biexciton (Δ_{XX^0}).

Each anticrossing has a corresponding fine structure whose pattern provides a signature of the spin configurations. In the biexciton, the two e 's are spin paired in the bottom dot and thus e - h exchange is not present. The

spin structure arises from the two h 's and is qualitatively the same as if the e 's were not there. If both h 's are in the same dot (${}^{20}XX^0$), and we consider only the lowest orbital state (s-shell), the Pauli principle demands that there can be only a spin singlet state. On the other hand, if the h 's are each in a different dot (${}^{11}XX^0$) there will be a singlet and three triplet spin states. For large barrier width ($d \geq 4$ nm) the interdot h - h exchange is negligible, and the spin singlet and triplet states are degenerate at electric fields away from the anticrossing region. However, because tunneling conserves spin in the region of strong anticrossing only the interdot singlet configuration ${}_{\uparrow\downarrow,0}^{1,0}XX_S^0$ mixes with the intradot singlet ${}_{\uparrow,\downarrow}^{1,0}XX_S^0$, and the degenerate triplet states ${}^{20}XX_T^0$ pass through unaffected as shown in Fig 2(b). This is similar to the situation observed in transport experiments on the 2- e system [4, 5]. Mixing of the singlet states in the anticrossing region leads to an effective or “kinetic” [17] h - h exchange splitting between the singlet and the three degenerate triplets, even though interdot h - h exchange is negligible for wide barriers. This type of exchange, which is highly sensitive to the applied electric field through the resonant tunneling, underlies the possibility of externally manipulating the spin coupling [4].

A magnetic field will lift the degeneracy between the triplets. However, as we now show, this degeneracy can be lifted even at zero magnetic field if e - h exchange is present. This is the case when the QDM contains a charged exciton, X^+ or X^- . Then, kinetic h - h (e - e) exchange and e - h exchange are both present, and compete to determine the character of the spin state. In Fig. 3(a) the spectral pattern for the positive trion, X^+ , is shown. This pattern can be readily understood using the energy state diagrams in Fig. 3(b) of both the trion and the h that is left behind after recombination. We focus our discussion on the anticrossing pattern within the box in Fig. 3(a), in which an apparent triplet transition wiggles as it passes through the resonance.

At electric fields away from the anticrossing region intradot e - h exchange determines the spin structure. That is, as shown in Fig. 3(b), e - h exchange leads to a fine structure doublet with a splitting of $2J^{eh}$, much like the intradot X^0 case. The higher energy component consists of the e and one h in the bottom dot with spins antiparallel (${}_{\downarrow,\uparrow}^{1,0}X^+$, ${}_{\uparrow,\downarrow}^{1,0}X^+$), while the lower energy component consists of parallel e and h spin in the bottom dot (${}_{\uparrow,\downarrow}^{1,0}X^+$, ${}_{\uparrow,\uparrow}^{1,0}X^+$) [13, 18].

As the electric field is tuned through the X^+ anticrossing region, tunnel coupling with the ${}_{\uparrow\downarrow,0}^{1,0}X_S^+$ state (in which both h 's in the bottom dot must form a spin singlet) forces the spin states (${}_{\downarrow,\uparrow}^{1,0}X^+$, ${}_{\uparrow,\downarrow}^{1,0}X^+$) to form a h spin singlet-like state (${}_{\downarrow,\uparrow}^{1,0}X_S^+$) and a h spin triplet-like state (${}_{\downarrow,\uparrow}^{1,0}X_T^+$). This triplet would pass straight through the resonance (as with the biexciton) except that e - h exchange continues to couple it to the singlets, causing it

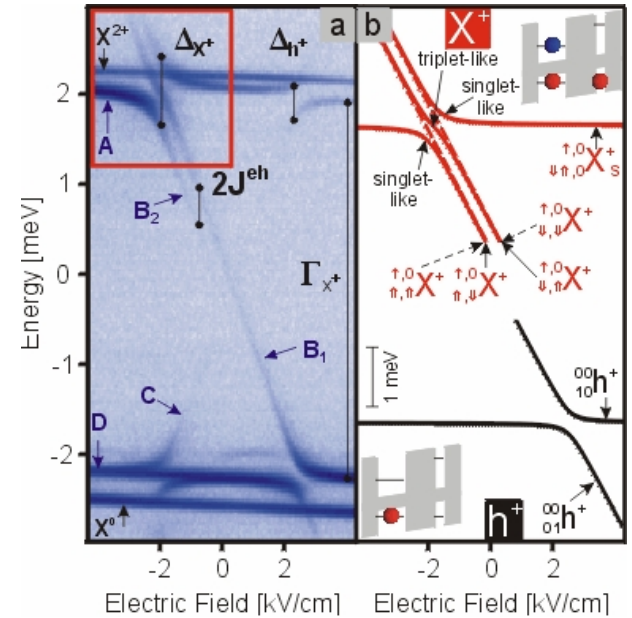


FIG. 3: (Color online) Positive trion (X^+) in a QDM ($h_B = h_T = 2.5$ nm, $d = 6$ nm). (a) In the measured PL spectrum as a function of electric field an ‘x’-shaped pattern is formed by the X^+ transitions ($A \equiv {}_{20}^{10}X^+$, $B \equiv {}_{11}^{10}X^+$, $C \equiv {}_{11}^{10}X^+ \rightarrow {}_{01}^{00}h^+$, $D \equiv {}_{11}^{10}X^+$). (b) The calculated level diagram contains the states of the positive trion (X^+) (red lines) and the states of a single hole (h^+) (black lines) ($\Delta_{h^+} = 2t_{h^+} = 390$ μ eV, $\Delta_{X^+} = 2\sqrt{2t_h^2 + (J^{eh})^2} = 780$ μ eV, $2J^{eh} = 450$ μ eV, $\Gamma_{X^+} = 4.16$ meV). The red box in (a) marks an area where the singlet-triplet mixing at the X^+ resonance in (b) is reproduced nicely by the PL-signal. In the lower left corner of (a) the anticrossing is reproduced by the transitions D and C with different intensity ratios, but is partially covered by ${}_{10}^{10}X^0$.

to shift continuously between the asymptotes determined by the e - h exchange splitting outside the anticrossing region. Essentially, in passing through the anticrossing region (from right to left) the ${}_{\downarrow,\uparrow}^{1,0}X^+$ state evolves continuously into the ${}_{\uparrow,\downarrow}^{1,0}X^+$ state through this triplet-like state. The Hamiltonian that describes this behavior of the states ${}_{\uparrow\downarrow,0}^{1,0}X_S^+$, ${}_{\downarrow,\uparrow}^{1,0}X^+$ and ${}_{\uparrow,\downarrow}^{1,0}X^+$ is [18]

$$\hat{H}_{\uparrow\downarrow}^{X^+} = \begin{pmatrix} E_{X^+} & t_h & t_h \\ t_h & E_{BT}^+ & 0 \\ t_h & 0 & E_{BT}^- \end{pmatrix}. \quad (3)$$

With energy and field relative to the anticrossing of the h states, E_{X^+} is the energy of ${}_{\uparrow\downarrow,0}^{1,0}X_S^+$, $E_{BT}^\pm = E_{X^+} - \Gamma_{X^+} \pm J^{eh} - \gamma F$ are the energies of the states ${}_{\downarrow,\uparrow}^{1,0}X^+$ and ${}_{\uparrow,\downarrow}^{1,0}X^+$, and Γ_{X^+} is the energy difference of the direct transitions A and D as defined in Fig. 3. Tunneling and e - h exchange lead to a measured anticrossing energy $\Delta_{X^+} = 2\sqrt{2t_h^2 + (J^{eh})^2}$. The remaining h spin triplet states (${}_{\downarrow,\downarrow}^{1,0}X^+$, ${}_{\uparrow,\uparrow}^{1,0}X^+$) retain their character and pass unaffected through the coupling region as

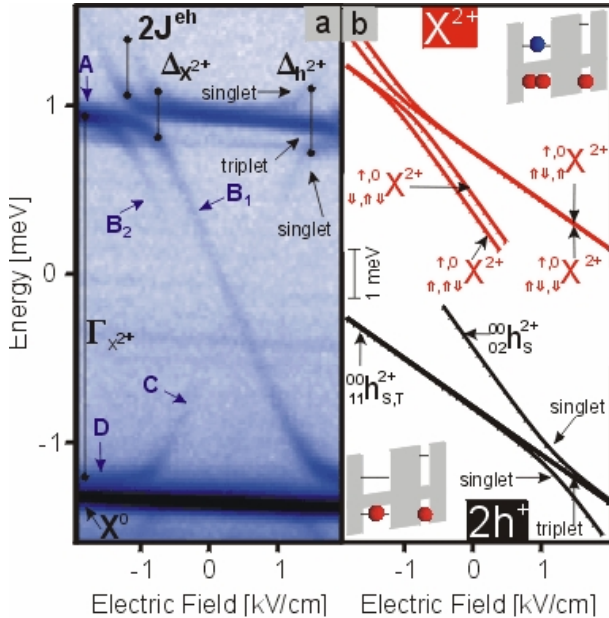


FIG. 4: (Color online) Doubly positively charged exciton (X^{2+}) in a QDM ($h_B = 4$ nm, $h_T = 2.5$ nm, $d = 4$ nm). (a) In the measured PL spectrum as a function of electric field an 'x'-shaped pattern is formed by the X^{2+} transitions ($A \equiv \frac{10}{21}X^{2+}$, $B \equiv \frac{10}{12}X^{2+}$, $C \equiv \frac{10}{21}X^{2+} \rightarrow {}^{00}h^{2+}$, $D \equiv \frac{10}{11}X^{2+}$). (b) The calculated level diagram contains the states of the doubly positively charged exciton (X^{2+}) (red lines) and the states of two holes (h^{2+}) (black lines) ($\Delta_{h^{2+}} = 2\sqrt{2}t_{h^{+}} = 410$ μ eV, $\Delta_{X^{2+}} = 2t_{h^{+}} = 310$ μ eV, $2J^{eh} = 370$ μ eV, $\Gamma_{X^{2+}} = 2.19$ meV).

shown in Fig. 3(b) (dashed lines), because Pauli blocking prevents the h 's from tunneling. Thus, at the anticrossing point there is a kinetic exchange splitting between singlet- and triplet-like states, as for the biexciton discussed above, but e - h exchange splits the degeneracy between the triplet states and leads to a mixing between the singlets and one of the triplets.

When the QDM is doubly charged we have the important case of a permanent two-spin system, where the lifetimes are not limited by radiative recombination. In this case we measure optically the doubly charged exciton X^{2+} . This state is especially interesting as an optical intermediary by which the two ground state spins can be measured or controlled. The spectral map measured for X^{2+} is shown in Fig. 4(a). The calculated level diagram that fits this spectrum is shown in Fig. 4(b).

The spin signatures within the X^{2+} spectral map are immediately understood by comparison with those of XX^0 . The h spin configurations of the final states in the X^{2+} transitions, ${}^{00}h^{2+}$ and ${}^{02}h^{2+}$, are equivalent to those of the biexciton initial states, ${}^{20}XX^0$ and ${}^{20}XX^0$, as can be seen by comparison of Fig. 4(b) and 2(b). Similarly, the spin configurations of X^{2+} are equivalent to those of X^0 , which are the final states of the biexciton transition. Thus, as can be seen by comparison of Figs.

4(a) and 2(a), the X^{2+} transition complex has spin features equivalent to that of XX^0 , but inverted.

An important implication of these results is that exchange is effectively turned off (or on) when the QDM is optically excited to specific spin states, thereby providing the opportunity for an ultrafast single qubit or 2-qubit operation. For example, the kinetic exchange interaction that splits the triplet and singlet states of the $2-h$'s, ${}^{00}h^{2+}$, could be 'optically gated' for a well defined time by driving the QDM up and down through a $\frac{10}{21}X^{2+}$ state (i.e. a virtual $\frac{10}{21}X^{2+}$ transition).

We have shown that the fine structure patterns measured in the optical spectra of QDMs are understood in detail in terms of the interplay between spin exchange and tunneling in the limit of wide barriers and negligible direct interdot exchange. Our description applies equally well to e tunneling and negatively charged QDMs. Interesting but more subtle effects such as fine structure due to asymmetries have for the most part remained below the resolution of our measurements.

We would like to acknowledge the financial support by NSA/ARO, CRDF, RFBR, RSSF, and ONR. M.F.D., I.V.P and E.A.S, are NRC/NRL Research Associates.

* Electronic address: scheibner@bloch.nrl.navy.mil

- [1] D. Loss, D.P. DiVincenzo, Phys. Rev. A **57**, 120 (1998).
- [2] D. P. DiVincenzo, *et al.*, Nature **408**, 339 (2000).
- [3] D. Awschalom, D. Loss and N. Samarth (eds.), *Semiconductor Spintronics and Quantum Computation* (Springer, 2002), ISBN 3540421769.
- [4] J. R. Petta, *et al.*, Science **309**, 2180 (2005).
- [5] F. H. L. Koppens, *et al.*, Science **309**, 1346 (2005).
- [6] D. Gammon, E. S. Snow, B. V. Shanabrook, D. S. Katzer, and D. Park, Phys. Rev. Lett. **76**, 3005 (1996).
- [7] B. Urbaszek, *et al.*, Phys. Rev. Lett. **90**, 247403 (2003).
- [8] H. J. Krenner, *et al.*, Phys. Rev. Lett. **94**, 057402 (2005).
- [9] G. Ortner, *et al.*, Phys. Rev. Lett. **94**, 157401 (2005).
- [10] E. A. Stinnett, *et al.*, Science **311**, 636 (2006).
- [11] Further details on the growth and the experimental methods can be found in Ref. [10].
- [12] K. V. Kavokin, Phys. Rev. B **69**, 075302 (2004).
- [13] $\frac{\uparrow,0}{\uparrow,\downarrow}X_{S(T)}^{+} \equiv \frac{1}{2} |B_1^h T_2^h \pm B_2^h T_1^h\rangle | \downarrow_1 \uparrow_2 \mp \downarrow_2 \uparrow_1 \rangle |B^e \uparrow\rangle$, where $B^{h(e)}$ and T^h denote the primary location of the orthonormal orbital wavefunctions of the e and the two h 's (1,2).
- [14] M. Bayer, O. Stern, A. Kuther, A. Forchel, Phys. Rev. B **61**, 7273 (2000).
- [15] For wide barriers contributions to the tunneling rate due to the presence of additional charges are negligible.
- [16] G. Burkard, G. Seelig and D. Loss, Phys. Rev. B **62**, 2581 (2000).
- [17] P. Fazekas, *Lecture Notes on Electron Correlation and Magnetism* (World Scientific, Singapore, 1999).
- [18] We define: $\frac{\uparrow,0}{\uparrow,\downarrow}X^{+} = \frac{1}{\sqrt{2}} (\frac{\uparrow,0}{\uparrow,\downarrow}X_S^{+} + \frac{\uparrow,0}{\uparrow,\downarrow}X_T^{+})$ and $\frac{\uparrow,0}{\uparrow,\downarrow}X^{+} = \frac{1}{\sqrt{2}} (\frac{\uparrow,0}{\uparrow,\downarrow}X_S^{+} - \frac{\uparrow,0}{\uparrow,\downarrow}X_T^{+})$.